Fracture Toughness Study of a Grade 300 Maraging Steel Weld Joint

Plane strain fracture toughness is determined directly from welded joints while weld simulation specimens add correlative data

BY J. G. BLAUEL, H. R. SMITH AND G. SCHULZE

ABSTRACT. The plane strain fracture toughness (K_{Ic}) of a gas tungsten-arc (GTA) welded joint prepared from 10 mm (0.39 in.) thick, grade 300, maraging steel was determined. Transverse three-point bend specimens, 10 × 10 × 55 mm (0.39 × 0.39 × 2.17 in.), were prepared with notches and precracks preferentially located in the weld and the heat-affected zone (HAZ), the outline of which had been revealed by prior polishing and etching. All critical K_I values less than about 270 kp mm$^{-3/2}$* (76 ksi-in.$^{1/2}$) satisfied ASTM validity criteria for K_{Ic}; these included determinations for all microstructures except one that was characterized by a very high stable austenite content.

The effect of microstructural and property variations characteristic of the HAZ on the determination of K_{Ic} was studied using "weld simulation" specimens thermally treated in a Smit weld simulator. Results were correlated with those obtained from actual welds on the basis of equivalent microstructures, mechanical properties, and thermal treatments. From this study, a tendency towards embrittlement due to short time exposure at 750 C was detected. It was also noted that K_{Ic} appeared to be independent of grain size.

Typical K_{Ic} values of the weld joint were as follows: for the base material: 250 kp mm$^{-3/2}$ (71 ksi-in.$^{1/2}$) for the high austenite zone: greater than 290 kp mm$^{-3/2}$ (82 ksi-in.$^{1/2}$) for the transformed zone: 230 kp mm$^{-3/2}$ (65 ksi-in.$^{1/2}$) and for the weld: 190 kp mm$^{-3/2}$ (54 ksi-in.$^{1/2}$).

**kp = kilopond, a unit of force exactly equal to the kilogramforce (kgf), is frequently used in Europe but is relatively unknown in the United States. In this paper, all expressions involving the kilopond have been converted to, and are followed by, U.S. customary units in parentheses — ed.*

J. G. BLAUEL and H. R. SMITH are with Institut für Festkorpermechanik der Fraunhofer Gesellschaft e.V., Freiburg, and G. SCHULZE is with Schweisstechnische Lehr-und Versuchsanstalt, Berlin, West Germany.

Introduction

There is a continuing demand for ultra high strength materials for application in weight critical structures. For example, most commercial and military aircraft use these materials in landing gears and other secondary structure. In most cases the designs require that the materials be heat treated to a strength level near that which is the maximum obtainable, a condition which unfortunately is also quite brittle. The designer is allowed to take a calculated risk concerning the possibility of brittle fracture because the failure of a secondary structure is not necessarily followed by catastrophic failure of the aircraft.

However, these risks can be minimized by a thorough understanding of the nature of the brittle fracture characteristics of the material — especially under welding conditions. In this regard, the tools provided by fracture mechanics can be utilized.

A number of workers have reported the results of fracture toughness testing of weld joints (Refs. 1-5). However it should be stated that extreme analytical and experimental difficulties in obtaining valid and meaningful results are introduced by the variation in microstructural properties and the operation of residual stresses resulting from the complex temperature profiles attending the multipass welding. A solution for the material part of this problem can be approached through augmenting the information derived from weld joint tests by use of a weld simulator (Refs. 6,7). In such an apparatus, localized regions of the heat-affected zone can be synthesized in cross sectional areas large enough to yield valid test results.

One of the more attractive weldable (Refs. 7,8,9), ultra high strength materials available today is maraging steel. It can be fabricated in a relatively soft solution annealed condition to final dimensions, and then aged to full hardness. The aging process involves the precipitation of intermetallic compounds in an essentially carbon free matrix at relatively low temperatures (450-500 C) with no accompanying phase transforma-

Fig. 1 — Microstructure of grade 300 maraging steel after hot-rolling, solution annealing at 820 C for 4 h, and aging at 480 C for 4 h. An extremely nonuniform structure due to incomplete recrystallization is indicated. (Electrolytic etch with 10% Cr_2O_3; X100, not reduced)

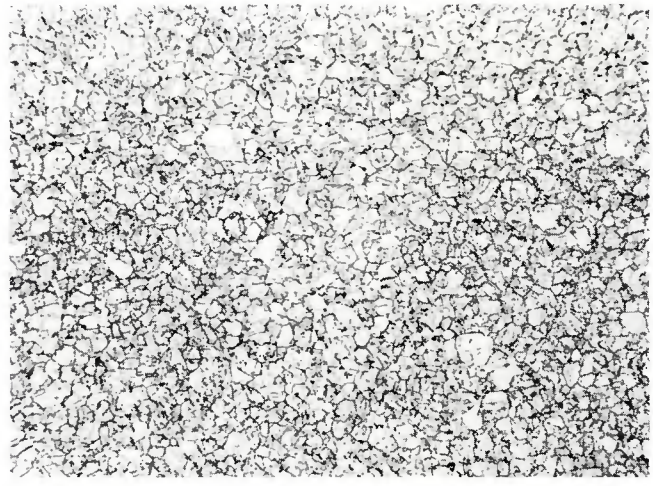

Fig. 2 — The material shown in Fig. 1 after an additional solution annealing treatment at 900 C for 4 h. Recrystallization is complete. (Etch and magnification same as Fig. 1)

Table 1 — Composition of Base and Filler Metals for X2 NiCoMo 18 9 5, wt%

	C	Si	Mn	P	S	Al	Co	Mo	Ni	Ti
Base metal	0.004	0.02	0.02	0.005	0.004	0.085	9.05	4.94	17.8	0.79
Filler metal	0.004	0.02	0.02	0.006	0.006	0.120	8.80	4.80	18.2	0.98

Table 2 — Mechanical Properties and Toughness of X2 NiCoMo 18 9 5 material

Ultimate tensile strength, σ_2 , kp/mm² (ksi)	216	(303)
Yield strength, σ_y , kp/mm² (ksi)	210	(299)
Fracture toughness, K_{Ic} , kp - mm $^{3/2}$ (ksi-in. $^{1/2}$	246	(69)
Vickers hardness, HV 50, kp/mm² (ksi)	610	(867)

tions. These features minimize the problems of dimensional stability, distortion, surface oxidation and decarburization commonly associated with quenched and tempered steels.

Depending on its composition, maraging steel can be aged to strength levels ranging from 140 to 240 kp/mm² (200 to 340 ksi) at toughness levels high in comparison to corresponding steels. For this reason maraging steel in the 190-210 kp/mm² (270-300 ksi) yield strength range was chosen as the research material of this program.

Material, Apparatus and Procedure

Material

The material was X2 NiCoMo 18 9 5 steel supplied by Stahlwerke Südwestfalen, Geisweid, and identified by their tradename as HFX 760. This material corresponds to American grade 300 18% Ni maraging steel. It was first prepared as a vacuum induction melted and electron-beam remelted 260 mm (10.24 in.) round block, which was subsequently hot rolled to a 10 mm thick plate and solution annealed at 820 C for ½ h. When aged at 480 C for 4 h, the material's microstructure appeared as in Fig. 1. This was considered to be too nonuniform to permit sensitive measurements of the grain size in the HAZ of a welded specimen, and consequently the material was resolution annealed at 900 C for ½ h. This resulted in the fine grained uniform microstructure shown in Fig. 2, which was then considered satisfactory for subsequent investigations.

The chemical composition is shown in Table 1, while mechanical properties and toughness of the reannealed material in the aged condition are shown in Table 2. From this point on, whatever prior processing (i.e., welding or simulation) was involved, specimens were subsequently aged at 480 C for 4 h.

Heat Treatment

At temperatures higher than 750 C, 18% nickel maraging steel (nominally 18% Ni, 9% Co, 5% Mo) exists as a face centered cubic, single phase austenite. On cooling, the austenite transforms by shear to body centered cubic martensite, irrespective of cooling rate. The low carbon Fe-Ni-martensite so formed is soft and ductile. On reheating in the 450-550 C range the alloy is hardened by the precipitation of intermetallic phases as Ni_3Mo and Ni_xTi_y (Refs. 10, 13). Optimum hardness is obtained by aging from 3 to 8 h in this range. However, after prolonged exposure, the alloy overages by a process involving reversion of the martensite to austenite, probably in the regions immediately surrounding the intermetallic compounds (Ref. 11). At higher temperatures (but still below 750 C), there is a tendency for the elements Ni and Ti to partition to the extent that a Ni-rich phase is retained on cooling to room temperature. It has been reported that the tendency to form stable austenite is strongest at 650 C (Refs. 12, 13), and at this temperature the required times are very short (of the order of seconds) (Refs. 14, 15). Furthermore, heating rate, hold time, and the number of overlaying cycles play important parts in the process (Ref. 15). These points are important in understanding the microstructure of a HAZ that must experience brief exposures to such conditions.

Welding

It has been demonstrated that the arc welding methods employing inert, protective gas produce sound joints of superior strength and toughness in maraging steel. Of these, the gas tungsten-arc welding (GTAW) process is easiest to control with respect to critical welding parameters.

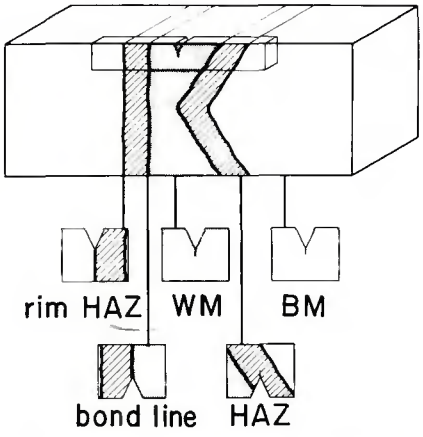

Fig. 3 — K configuration weld joint showing specimen and notch locations. BM = base metal, WM = weld metal zone, HAZ = heat-affected zone

Table 3 — Parameters for GTA Welding — by Passes

Parameter	Pass number 1	2	3	4	5	6
Current, A	195	210	210	230	210	210
Voltage, V	13	15	15	15	15	15
Welding speed, cm/sec,	0.18	0.18	0.13	0.18	0.18	0.09
in./min	4.2	4.2	3.1	4.2	4.2	2.1
Energy input, kJ/cm,	14.1	17.6	24.2	19.2	17.6	35
kJ/in.	35.8	44.7	61.5	48.8	44.7	88.9

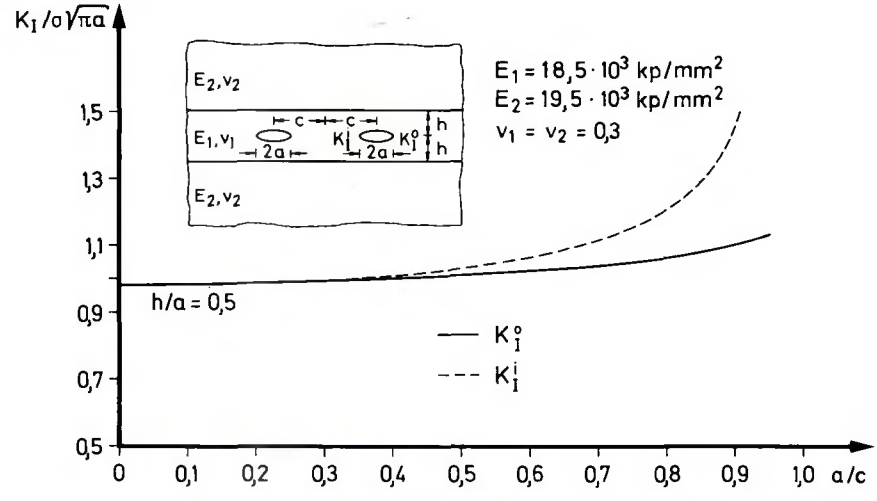

Fig. 4 — Stress intensity factors for coplanar cracks located in a layered medium (Ref. 19)

Accordingly, the GTAW process was chosen to weld the K-configuration joints shown in Fig. 3. The welding was parallel to the rolling direction. The HAZ that forms on the straight, perpendicular wall of the joint has itself straight boundaries. This facilitates the location of the notch and precrack in subsequently fabricated test specimens. The plates were hand welded with multiple passes using the parameters shown in Table 3. The filler metal (2 mm or 0.079 in. diam) composition is shown in Table 1. Radiographically acceptable welds were obtained when exceptional measures were taken to maintain cleanliness from pass to pass. (Ref. 16).

Weld Simulation

A Smit weld simulator (Ref. 17) was employed to synthesize localized HAZ microstructures in the cross section of test specimens by controlled resistance heating and water cooling. Reference cycles were obtained by running a bead on the surface of a plate, and recording the temperature as a function of time at various selected distances from the weld fusion line. These reference cycles, in turn, provided a basis for constructing simple treatments that would simulate the effect imposed by single pass welding. Peak temperatures of 650, 700, 750, 800, and 1350 C were selected on the basis of microstructural analysis as those best suited to provide a critical survey of the strength and toughness behavior of the HAZ.

The temperature history for each simulation specimen was controlled by a thermocouple spot welded to the surface at the middle of its length. Although there was a considerable gradient from end to end, the temperatures in the surface-to-surface planes were uniform. The phase transformations occuring in each treatment were measured *in situ* by a dilatometer.

Fracture Mechanics in Relation to the Weld Joint

In an elastic, isotropic, and homogenous medium containing a crack, the stress intensity factor K for mode I loading is given by:

$$K_I = \sigma (\pi a)^{1/2} Y \qquad (1)$$

where σ is the gross section stress, a is the crack length, and Y is a factor which accounts for the boundary influences associated with a particular configuration and loading mode (in this program, a three point bend system was used).

In performing a fracture toughness test, a specimen containing a well defined fatigue precrack is loaded to failure. According to fracture mechanics, the criterion for failure is described in terms of a critical stress intensity level with respect to the material. This is defined as the material's fracture toughness. When constraint to deformation at the crack tip is severe enough to approximate closely the plane strain state of stress, the critical stress intensity factor is called K_{Ic}. The procedure in determining a valid value for K_{Ic} has been specified by ASTM (Ref. 18). Under the conditions of this specification, the value so determined is independent of geometry, and consequently, it is desirable whenever possible to evaluate toughness in terms of K_{Ic}.

When the principles of fracture mechanics are applied to the study of a weld joint, the degree of microstructural anisotropy and the state of residual stress in the joint must be considered.

The effect of anisotropy on the stress distribution at the crack tip can be examined by referring to simple cases which can be handled analytically. In Fig. 4, for example, the stress intensity solutions for a system for two coplanar cracks are shown contained in a layered medium in which the elastic constants are typical for different zones of the weld joint (Ref. 19). The stress intensity factor K_I^i pertains to the inner tips, while K_I^o applies to the outer tips of the cracks. When the cracks lie far apart (in Fig. 4 this corresponds to small values of a/c) there is no interaction of the stress fields. K and K_I^o become identical, and the representation is that of a single crack. K_I for the layered medium is normalized by $\sigma (\pi a)^{1/2}$, the value of K for a homogeneous medium, to permit direct observation of the anisotropic influence. It can be seen that for the given difference in elastic constants of the var-

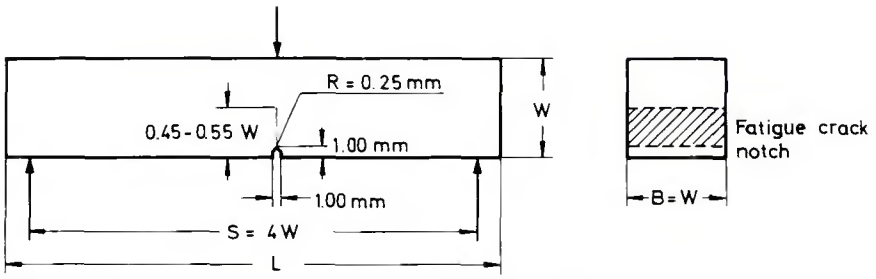

Fig. 5 — Three point bend specimens for K_{Ic} determination

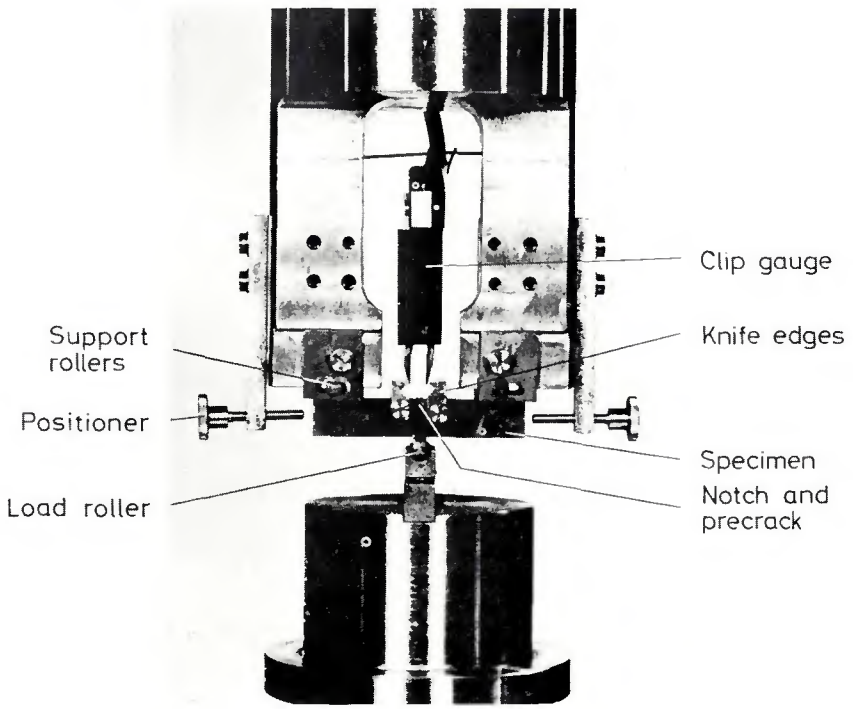

Fig. 6 — Three point bend testing fixtures

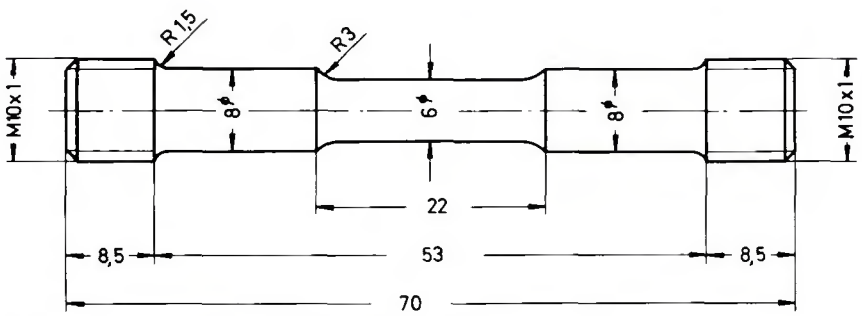

Fig. 7 — Round bar tensile specimen with double reduced section

ious microstructures represented in the HAZ of maraging steel, the ratio of $K_I / \sigma\ (\pi a)^{1/2}$ is only about 2 or 3% less than one. It is concluded from this and further analytical results (Ref. 19) that the linear elastic stress analysis for an isotropic and homogeneous medium is still appropriate.

When determining critical stress intensity levels (K_{Ic}) as material values, the influence of the anisotropy and inhomogenity on the formation of the plastic zone at the crack tip must also be considered. The size of the plastic zone influences the fracture toughness, i.e., the resistance against instable fracture, and that, in turn, can be defined as a function of the ratio of the elastic stress intensity factor K_{Ic} to an effective local yield strength which takes into account the differing plastic deformation behavior of the various microstructures and their interaction. In this program representative values of σ_y for local yield strength (0.2% offset in uniaxial tension) were determined from round-bar tension experiments and used to check the validity criteria for K_{Ic} measurements (see also later).

With respect to residual stress it has been shown that the following observations are pertinent to maraging steel welds (Ref. 20):

(1) The residual stress is dominant in the longitudinal direction (i.e. parallel to the weld); however, transverse residual stress at a much lower level also is developed.

(2) The residual stress is compressive along the weld centerline, balanced by tensile stresses in the HAZ on each side.

All the specimens are taken transverse by cutting at right angles to the weld length. Their cracks are extended in a direction through the thickness of the plate and in a plane parallel to the weld length (Fig. 3). Then only the minor transverse residual stresses can superpose on the external applied stress, and they will add or subtract according to their distribution indicated in (Ref. 2). However, their influence was not apparent when driving the fatigue crack through different zones of the weld. It is generally known that cutting the weld length in segments, as is done in preparing the small transverse test specimens, should lower the residual stress level.

In summary, it appeared that the influence of residual stress on the results of the program was insignificant.

Evaluation of Strength, Toughness and Microstructure

To evaluate K_{Ic}, three point bend specimens as depicted in Fig. 5 were chosen. A preliminary program indicated that specimens taken transverse to the rolling direction with precracks directed through the thickness gave rise to the lowest fracture toughness values. All subsequent bend specimens were fabricated in this manner. Generally, the specimens were prepared to final dimensions (with chevron or straight notch) when the material was in the soft solution-annealed condition. They were then aged and fatigue precracked prior to testing. In the case of the weld specimens, however, it was necessary to first prepare the specimens to rough dimensions only. Then, one of the side surfaces of each was polished and etched to reveal the weldment and HAZ. The position of the notch was located as desired, and then the preparation was continued as for the unwelded specimens.

The specimen size (i.e. width and thickness) was limited by what could be treated in the Smit simulator. Thus, the width-thickness dimensions for all specimens were 10 × 10

mm with the precrack length being 5 mm. The load fixtures were arranged so that specimens of all lengths could be tested; however, the major span length for each was 40 mm (1.58 in.). A clip gauge was designed to fit into knife edges mounted on the specimen adjacent to the notch. The assembled apparatus is shown in Fig. 6. Load-displacement curves obtained from the tests were used to calculate K_{Ic} in accordance with the specified procedure (Ref. 18).

The restrictions on specimen dimensions governing the determination of K_{Ic} are given by:

$$a, B \geq 2.5 (K_{Ic} / \sigma_Y)^2 \qquad (2)$$

where a is crack length, B is thickness, and σ_Y is the "effective" material's yield strength. With a limiting crack length of 5 mm, the maximum valid K_{Ic} that could be measured was about 270 kp-mm$^{-3/2}$ (76 ksi-in.$^{1/2}$) when the lower limiting yield strength was 190 kp/mm^2 (270 ksi).

Tensile tests were performed using the specimen shown in Fig. 7. In consideration of the simulation treated specimens, the design was arranged such that the 690 C isotherm was always located in the lower-stressed shoulder of the reduced section. This is important due to the tendency for soft austenite to form and stabilize at this temperature. It was necessary to use longitudinal specimens to determine the strength of the weldment and the transformed zone immediately adjacent to it in an actual weld. Vickers hardness was also measured for each zone of interest.

The most important microstructural features were considered to be the prior austenitic grain size and the percentage of retained austenite. These were measured on the carefully ground and polished fracture surfaces of broken bend specimens. Electrolytic etching with 10% Cr_2O_3 revealed the prior austenitic grain outline quite clearly if the structure had first been age hardened. Ordinary etching with V2A Beize (50 ml HCl, 5 ml HNO_3, 0.15 ml Sparbeize inhibitor) developed the austenitic-martensitic microstructure and it was found that overlaying the second treatment on the first produced a microstructure in which all the salient features could be seen. Additionally, retained austenite content was measured by x-ray diffraction (Ref. 21). Grain size was determined by the intercept method in the prescribed manner (Ref. 22).

Results and Discussion

The weld joint was analyzed in terms of three areas of interest: (1) the weld metal zone, (2) the transformed zone, and (3) the dark etching zone. The microstructures and properties of these areas are compared with those of the simulation treated material in Figs. 8,9. The weld metal zone of the joint is seen in Fig. 12.

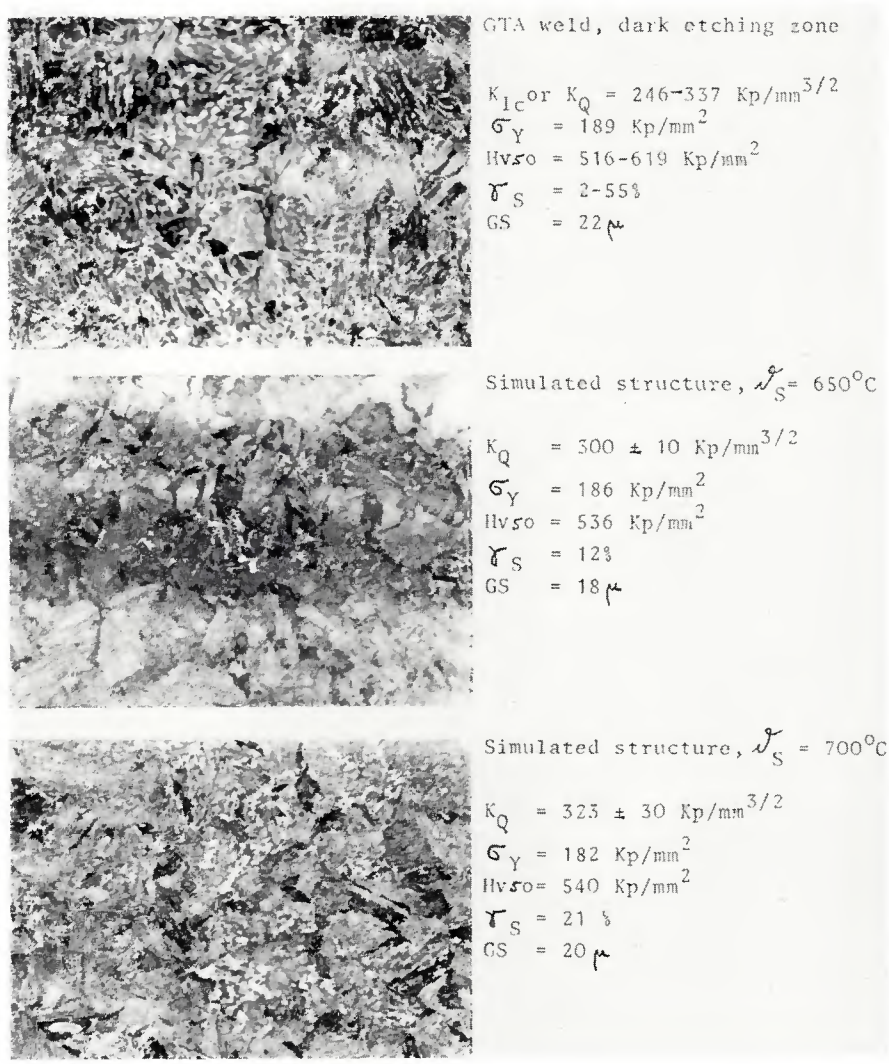

Fig. 8 — Microstructures and properties of simulated structures compared with the dark etching zone of a GTA weld. (Etch: electrolytic with 10% Cr_2O_3 + V2A Beize; X500, reduced 35%)

ϑ_S = peak temperature of simulation cycle
K_Q = fracture toughness not fulfilling all ASTM specifications
σ_y = yield strength
Hv50 = Vickers hardness, load 50 kp
γ_S = weight percent of retained austenite
GS = prior austenitic grain size

The dark etching zone is characterized by high stable austenite (γ_s) content distributed in a thin band at the "cold" edge of the transformed zone. Such a distribution influences the accuracy of the determination, and the percentages reported must be considered as approximate. The γ_s gradient was severe, varying from 0 to 50% in about 3 mm. The 650 and 700 C simulation treatments developed structures which corresponded with the weld's dark etching zone. However, the γ_s contents were uniform in and around the central cross section of the specimen, and the overall levels were lower at 12 and 21% respectively. The higher level coming from the 700 C treatment is reasonable since the dilatometer information for all treatments showed a sharp phase change at 690 C.

The area between the dark etching and weld metal zones consisted of transformed and recrystallized martensite containing virtually no retained austenite. The prior austenitic grain size varied from about 24 μ at the edge of the dark band to about 50 μ near the fusion line. The 750 and 800 C simulation treatments produced microstructures comparable to those seen in the recrystallized zone near the dark band, with the grain size being 24 and 26 μ respectively. Some γ_s in the amounts of 8% for the 750 C treatment and 5% for the 800 C treatment were measured, in contrast to the recrystallized zone. The 1350 C treatment developed a structure similar to the HAZ near the

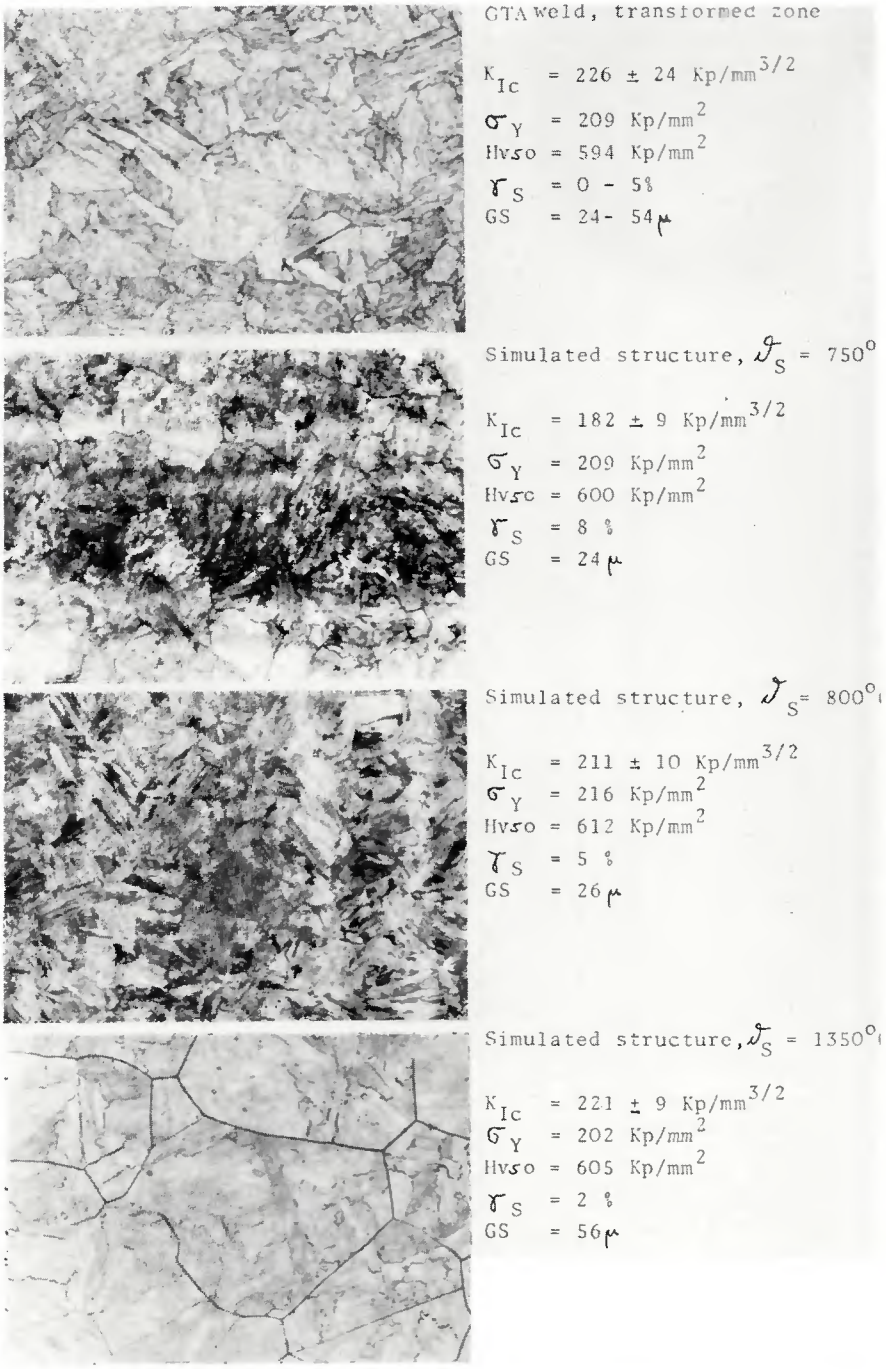

Fig. 9 — Microstructures and properties of simulated structures compared with the transformed zone of a GTA weld. (X500, reduced 35%)

bond line, the grain size being 56 μ and the γ_s content less than 2%. The weld metal zone of the joint consisted of dendrites of transformed martensite containing a dispersion of γ_s pools.

The plane strain fracture toughnesses reported for all structures except those containing high γ_s contents are valid in accordance with ASTM specifications, and are identified as K_{Ic} in Figs. 8-11. Values reported as K_Q in these figures are considered to be invalid only because the crack lengths were slightly too short, and they may be treated as good estimates of K_{Ic}.

The number of tests was 5 as a minimum for uniform structures and between 10 and 20 for the weld structures zones. In the figures mean values are given together with their standard deviation.

Figure 12 shows a typical example of a load-displacement curve of a fracture mechanics test together with views of the fracture surface and the corresponding microstructure.

Concerning the dark etching part of the HAZ, it was very difficult to locate precracks from specimen to specimen in zones of equal γ_s content due to the steep concentration gradient noted above. This gave rise to scattered K_Q results, a detraction that was not observed in the simulation specimens. This serves to emphasize the importance of the weld simulation approach as an adjunct to direct testing of a weld joint.

It can be seen from Figs. 8-11 that of all the structures represented in the weld joint, that of the weld metal zone is the most brittle, in spite of its low yield strength. However, the weld metal was largely ignored because its properties can be controlled by the filler metal composition. The dark etching zone developed fracture toughnesses varying from 246 to 337 kp-mm$^{-3/2}$ (69-95 ksi-in$^{1/2}$). The simulation results indicate that γ_s contents as low as 12% can elevate the fracture toughness significantly, which is in direct contrast to the weld metal zone results. It has been reported that the morphology of γ_s in maraging steel exerts an important influence on fracture toughness (Ref. 4). The point could not be pursued in this program because the martensite matrix of the weld metal was harder than that of the dark etching zone probably as a result of the higher Ti content due to the filler metal composition.

It is interesting to note that although the precrack location in specimens coming from the recrystallized part of the HAZ was random with respect to grain size, the K_{Ic} scatter was negligible. A detrimental influence of increasing grain size on K_{Ic} is not apparent, an observation supported by the results of the 750, 800 and 1350 C simulation treatments. This may be due to the fact that the overlying martensitic structure was uniform in size irrespective of the prior austenitic grain size.

A metallurgical effect of as yet unknown origin appears to be influencing the toughness of the 750 C treatment.

It can be seen in Fig. 10 that the K_{Ic} value is significantly lower than those of the other treatments and that of the base metal.

Conclusions

The following conclusions can be drawn regarding the fracture mechanics analysis of a GTA welded joint of a grade 300 maraging steel:

1. The plane strain fracture toughness K_{Ic} can be determined directly from the weld joint; however, weld simulation specimens offer an extremely valuable supplement to any such testing program.

2. Concentrations of retained austenite ranging to 50% are found in a narrow region of the HAZ, apparently

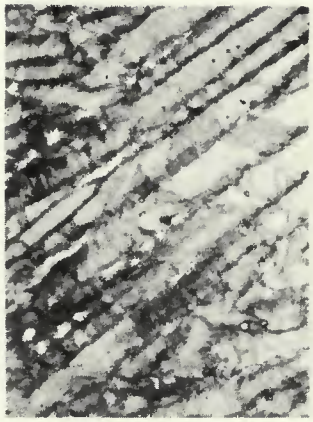

K_{Ic} = 190 ± 15 Kp/mm$^{3/2}$
σ_Y = 181 Kp/mm^2
Hv$_{50}$ = 588 Kp/mm^2
γ_S = 9,4 %

Fig. 10 — Weld metal zone microstructure and properties (Etch: electrolytic with 10% Cr_2O_3 + V2A Beize; X500, reduced 18%)

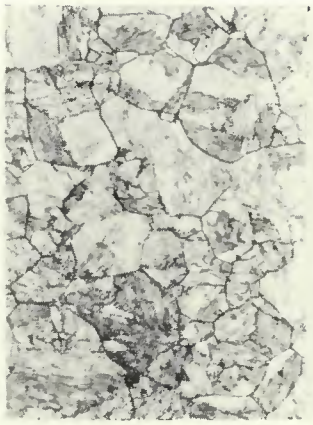

K_{Ic} = 246 ± 8 Kp/mm$^{3/2}$
σ_Y = 210 Kp/mm^2
Hv$_{50}$ = 610 Kp/mm^2
γ_S = 2 %
GS = 18 - 22 µ

Fig. 11 — Base metal microstructure and properties (Etch: electrolytic with 10% Cr_2O_3 + V2A Beize; X500, reduced 18%)

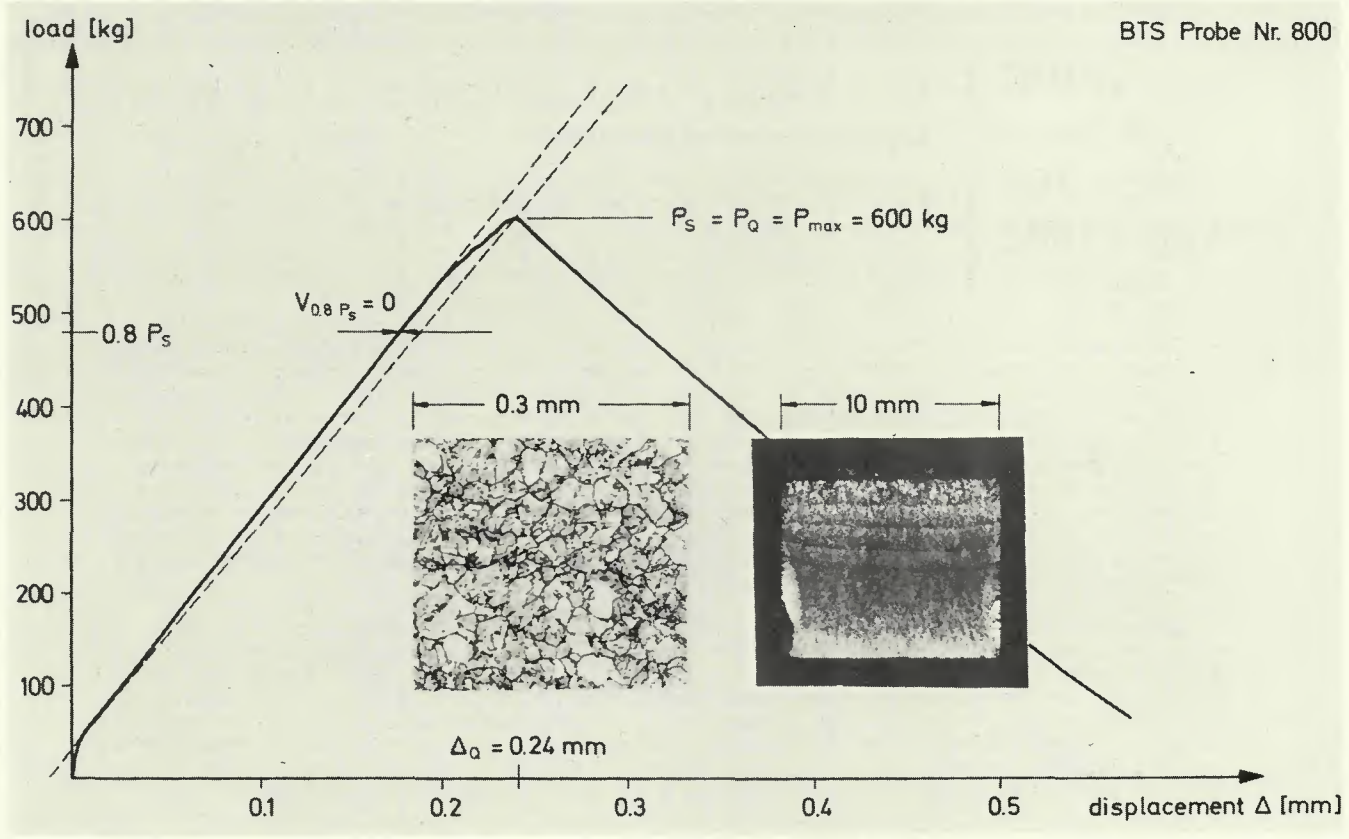

Fig. 12 — Load-displacement curve of a fracture mechanics test of the transformed structure in the HAZ of a GTA weld, together with the microstructure in the region of the fatigue crack tip and a macrograph of the crack surface

as a result of repeated very short time exposure to temperatures between 650 and 700 C. The fracture toughness K_{Ic} in this zone is elevated significently, but the attendent lowering of yield strength is not serious.

3. Prior austenitic grain size in the recrystallized portion of the HAZ does not influence K_{Ic} .

4. A possible embrittling effect is associated with planes of the HAZ experiencing short time exposure to 750 C.

Acknowledgement

The work for this program was performed under the auspices of the Deutscher Verband fur Schweisstechnik (DVS). We wish to thank the Arbeitsgemeinschaft Industrieller Forschungsvereinigungen (AIF) for financial support.

References

1. Bailey, N. "Weldability and Toughness of Maraging Steel", *Metal Construction British Welding Journal,* Vol. 3, pp 1-5, 1971.

2. Cottrell, C. L. M. "Fracture Toughness Concepts Applied to the Zones of Welded Joints", *British Welding Journal,* Vol. 15, 262-267, 1968.

3. Kies, J. A., Smith, H. L., Romine, H. "Fracture Toughness and Critical Defect Sizes With Welds of 18% Nickel Maraging Steels", *Metals Engineering Quarterly,* Vol. 6, 37-47, 1966.

4. Salmon-Cox, P. H., Birkle, A. J., Reisdorf, B. G., Pellisier, G. E. "An Investigation of the Mechanical Properties and Microstructure of 18 Ni (250) Maraging Steel Weldments", *Transactions, ASM Quarterly,* Vol. 60, 1967.

5. Weiss, B. Z., Steffens, H. D., Seifert, K. "Fracture Toughness of the Heat Affected Zone in 14 Cr Mo V 69 Steel and 18 Ni Maraging Steel", *Welding Journal,* Vol. 51, 9, (Sept.) 1972, Research Suppl., pp. 449-s to 456-s.

6. Pepe, J. J., Savage, W. F., "The Weld Heat Affected Zone of the 18 Ni Maraging Steels", *Welding Journal,* Vol. 49, no. 12 (Dec.) 1970 Research Suppl., pp. 454-s to 553-s.

7. Lang, H. J., Kenyon, N. "Welding of

Maraging Steels" Welding Research Council Bulletin 159, 1971.

8. Canonico, D. A., "Gas Metal Arc Welding of 18% Nickel Maraging Steel", *Welding Journal,* Vol. 43, no. 10 (Oct.) 1964, Research Suppl., pp. 433-s to 442-s.

9. Adams, C. M. Jr., Travis, R. E., "Welding of 18% Ni-Co-Mo Maraging Alloys", *Welding Journal,* Vol. 43, no. 5 (May) 1964, Research Suppl., pp. 193-s to 197-s.

10. Baker, A. J., Swann, P. R. "The Hardening Mechanism in Maraging Steels", *ASM Transactions,* Vol. 57, pp. 1008-1011, 1964.

11. Reisdorf, B. G., Baker, A. J. "The Kinetics and Mechanisms of the Strengthening of Maraging Steels", Technical Report AFML - TR - 65-390, 1965.

12. Peters, D. T. "A Study of Austenite Reversion during Aging of Maraging Steels", *ASM Transactions,* Vol. 61, pp. 62-74, 1968.

13. Floreen, S. F. "The Physical Metallurgy of Maraging Steels", *Metallurgical Review,* Vol. 13, pp. 115-128, 1968.

14. Petersen, A., "Weld Heat Affected Zone of 18% Nickel Maraging Steel", *Welding Journal,* Vol. 43, no. 9 (Sept.) 1964, Research Suppl., pp. 428-s to 432-s.

15. Goldberg, A., O'Connor, D. G., "Influence of Heating Rate on the Transformation of an 18% Nickel Maraging Steel", *Nature,* Vol. 213, pp. 170-171, 1967.

16. Blauel, J. G., Smith, H. R., Schulze, G., "Messung der Riss-zahigkeit an Schweissverbindungen und thermisch simulierten Gefügen aus einem martensitaushärtbaren Stahl", Report no. 4/73, Institut für Festkörpermechanik, Freiburg, 1973.

17. Adrichem, T. I., Kas, I. "Calculation, Measurement and Simulation of Weld Thermal Cycles", Company Report of Smit-Weld, N.V. Nijmwegen, Holland, 1969.

18. ASTM-Designation E 399-70 T, "Tentative Method of Test for Plane Strain Fracture Toughness of Metallic Materials", *ASTM Book of Standards,* Part 31, 1970.

19. Ratwani, M., "Wechselwirkung von Rissen", Report 5/72, Institut fur Festkörpermechanik, Freiburg, 1972.

20. Adams, Jr. C. M., Corrigan, D. A., "Mechanical and Metallurgical Behavior of Restrained Welds in Submarine Steels", MIT Final Report on Contract No. NObs - 92077, 1966.

21. Averbach, B. L., Cohen, M., "X-ray Determination of Retained Austenite by Integrated Intensities", *Transaction of AIME,* Vol. 176, pp. 401-414, 1948.

22. ASTM-Designation E 112-4, "Average Grain Size of Metals", *ASTM Book of Standards,* Part 31, 1969.

WRC Bulletin No. 107 Aug. 1965

(Reprinted April 1972)

Local Stresses in Spherical and Cylindrical Shells Due to External Loadings

by K. R. Wichman, A. G. Hopper and J. L. Mershon

Several years ago, the Pressure Vessel Research Committee sponsored an analytical and experimental research program aimed at providing methods of determining the stresses in pressure vessel nozzle connections subjected to various forms of external loading. The analytical portion of this work was accomplished by Prof. P. P. Bijlaard of Cornell University. Development of the theoretical solutions involved a number of simplifying assumptions, including the use of shallow shell theory for spherical vessels and flexible loading surfaces for cylindrical vessels. These circumstances limited the potential usefulness of the results to d_i/D_i ratios of perhaps 0.33 in the case of spherical shells and 0.25 in the case of cylindrical shells. Since no data were available for the larger diameter ratios, Prof. Bijlaard later supplied data, at the urging of the design engineers, for the values of $B = 0.375$ and 0.50 (d_i/D_i ratios approaching 0.60) for cylindrical shells. In so doing, Prof. Bijlaard included a specific warning concerning the possible limitations of these data.

Following completion of the theoretical work, experimental work was undertaken in an effort to verify the theory. Whereas this work seemingly provided reasonable verification of the theory, it was limited to relatively small d_i/D_i ratios—0.10 in the case of spherical shells and 0.126 in the case of cylindrical shells. Since virtually no data, either analytical or experimental, were available covering the larger diameter ratios, the Bureau of Ships sponsored a limited investigation of this problem in spheres, aimed at a particular design problem, and the Pressure Vessel Research Committee undertook a somewhat similar investigation in cylinders. Results of this work emphasized the limitations in Bijlaard's data on cylindrical shells, particularly as it applies to thin shells over the "extended range."

Incident to the use of Bijlaard's data for design purposes, it had become apparent that design engineers sometimes haye difficulty in interpreting or properly applying this work. As a result of such experience, PVRC felt it desirable that all of Bijlaard's work be summarized in convenient, "cookbook" form to facilitate its use by design engineers. However, before this document could be issued, the above mentioned limitations became apparent presenting an unfortunate dilemma, viz., the data indicate that the data are partially inadequate, but the exact nature and magnitude of the error is not known, nor is any better analytical treatment of the problem available (for cylinders).

Under these circumstances, it was decided that the best course was to proceed with issuing the "cookbook," extending Bijlaard's curves as best as possible on the basis of available test data. This decision was based on the premise that all of the proposed changes would be toward the conservative (or "safe") side and that design engineers would continue to use Bijlaard's extended range data unless some alternative were offered. This paper was therefore presented in the hope that it would facilitate the use of Bijlaard's work by design engineers.

Since the paper was originally issued, a number of minor errors have been discovered and incorporated in revised printings as supplies were exhausted. The third revised printing was issued in April 1972.

The price of Bulletin No. 107 is $3.00. Copies may be ordered from the Welding Research Council, 345 East 47th St., New York, N. Y. 10017.